A Single-Domain TCR-like Antibody Selective for the Qa-1(b)/Qdm Peptide Complex Enhances Tumoricidal Activity of NK Cells via Blocking the NKG2A Immune Checkpoint

Ghaffari, S.; Upchurch-Ange, K.; Gimlin, S.; Tripathi, T.; Sluijter, M.; Middelburg, J.; ... ; Weidanz, J.

The Journal of Immunology

RESEARCH ARTICLE | MAY 01 2022

A Single-Domain TCR-like Antibody Selective for the Qa-1^b/Qdm Peptide Complex Enhances Tumoricidal Activity of NK Cells via Blocking the NKG2A Immune Checkpoint

Soroush Ghaffari; ... et. al

J Immunol (2022) 208 (9): 2246–2255.
https://doi.org/10.4049/jimmunol.2100790

A Single-Domain TCR-like Antibody Selective for the Qa-1^b/Qdm Peptide Complex Enhances Tumoricidal Activity of NK Cells via Blocking the NKG2A Immune Checkpoint

Soroush Ghaffari,* Katherine Upchurch-Ange,† Susanne Gimlin,† Trivendra Tripathi,† Marjolein Sluijter,‡ Jim Middelburg,‡ Thorbald van Hall,‡ and Jon Weidanz†,§

The NKG2A/HLA-E axis is an immune checkpoint that suppresses immune effector activity in the tumor microenvironment. In mice, the ligand for the NKG2A/CD94 inhibitory receptor is the nonclassical MHC molecule Qa-1^b, the HLA-E ortholog, which presents the peptide AMAPRTLLL, referred to as Qdm (for Qa-1 determinant modifier). This dominant peptide is derived from the leader sequences of murine classical MHC class I encoded by the H-2D and -L loci. To broaden our understanding of Qa-1^b/Qdm peptide complex biology and its tumor protective role, we identified a TCR-like Ab from a single domain VHH library using yeast surface display. The TCR-like Ab (EXX-1) binds only to the Qa-1^b/Qdm peptide complex and not to Qa-1^b alone or Qa-1^b loaded with control peptides. Conversely, currently available Abs to Qa-1^b bind independent of peptide loaded. Flow cytometric results revealed that EXX-1 selectively bound to Qa-1^b/Qdm-positive B16F10, RMA, and TC-1 mouse tumor cells but only after pretreatment with IFN-γ; no binding was observed following genetic knockdown of Qa-1^b or Qdm peptide. Furthermore, EXX-1 Ab blockade promoted NK cell–mediated tumor cell lysis in vitro. Our findings show that EXX-1 has exquisite binding specificity for the Qa-1^b/Qdm peptide complex, making it a valuable research tool for further investigation of the Qa-1^b/Qdm peptide complex expression and regulation in healthy and diseased cells and for evaluation as an immune checkpoint blocking Ab in syngeneic mouse tumor models. ***The Journal of Immunology*****, 2022, 208: 2246–2255.**

The NKG2A axis is a novel immune checkpoint believed to control the cytolytic activity of effector cells in the tumor microenvironment (1, 2). Blocking this inhibitory pathway has been shown to promote anti-tumor immunity in cancer patients and in murine tumor models by enhancing the lysis activity of NK and CD8$^+$ T cells (3, 4). Findings from a recent phase II study showed clinical benefit in head and neck cancer patients treated with an anti-NKG2A Ab, monalizumab, in combination with cetuximab (anti-EGFR mAb) (3). Additionally, a mAb targeting mouse the NKG2A receptor has shown efficacy in murine tumor models when used in combination with PD-L1 therapy or cancer vaccines (3, 4). The ligand for the NKG2A/CD94 heterodimeric receptor in mice is Qa-1^b, the HLA-E ortholog.

The nonclassical MHC molecule (MHC class Ib), Qa-1^b, is an essentially monomorphic protein with similar tissue distribution as classical MHC class I molecules (MHC class Ia), albeit at lower levels (5, 6). The Qa-1^b molecule presents the dominant nonameric peptide AMAPRTLLL, referred to as Qdm (for Qa-1 determinant modifier), that is derived from the leader sequence of murine MHC class Ia from the H-2D and -L loci (7–9). Because Qdm peptide presentation by Qa-1^b directly correlates with MHC class Ia expression and Ag-processing machinery (APM) integrity, loss of either one results in the reduction or even absence of Qdm peptide, indicating that the display of Qa-1^b/Qdm complexes at the surface of cells can act as a barometer for MHC class Ia and APM integrity (10).

The inhibitory NKG2A receptor belongs to the NKG2 family of C-type lectin-like receptors that also includes two activating variants, NKG2C and NKG2E. NKG2 molecules pair with CD94 to form functional heterodimeric receptors that interact with Qa-1^b when complexed with Qdm (11, 12). Interaction of the NKG2A/CD94 heterodimeric inhibitory receptor to Qa-1^b or HLA-E molecules recruits SHP-1 (protein tyrosine phosphatase, non-receptor type 6 [PTPN6]) that promotes an inhibitory signaling cascade in the effector cells to suppress immune activities (13–15). In addition to NK cells, recent reports have shown that tissue-resident and tumor-localized CD8$^+$ T cells express the NKG2A/CD94 receptor at markedly higher frequencies compared with circulating CD8$^+$ T cells (16, 17). The currently held belief is that Qa-1^b engages with the NKG2A/CD94 inhibitory receptor when presenting the Qdm peptide to protect cells from lysis by NK cells (18–22).

Even though healthy cells are expected to express Qa-1^b loaded with Qdm peptide, during infections or in tumor cells alternative peptides can be presented by Qa-1^b molecules (9, 23). Currently, no distinction using Abs can be made between the different peptides, including Qdm, that are presented by Qa-1^b complexes in healthy and diseased cells. Novel research tools that could directly recognize the Qa-1^b/Qdm complex or Qa-1^b loaded with other peptides in normal or tumor tissue would be particularly useful. Such tools would be invaluable in furthering our understanding of Qa-1^b/Qdm expression and regulation in normal cells as well as in nonmalignant and malignant cells present in the tumor

*Department of Biology, College of Science, The University of Texas at Arlington, Arlington, TX; †Abexxa Biologics, Inc., Arlington, TX; ‡Department of Medical Oncology, Oncode Institute, Leiden University Medical Center, Leiden, the Netherlands; and §College of Nursing and Health Innovation, The University of Texas at Arlington, Arlington, TX

ORCIDs: 0000-0002-9813-3949 (K.U.-A.); 0000-0002-6006-1273 (T.T.); 0000-0002-4797-9653 (J.M.); 0000-0002-9115-558X (T.v.H.); 0000-0003-4455-9319 (J.W.).

Received for publication August 12, 2021. Accepted for publication February 17, 2022.

Address correspondence and reprint requests to Prof. Jon Weidanz, The University of Texas at Arlington, 701 S. Nedderman Drive, Arlington, TX 76019. E-mail address: weidanz@uta.edu

Abbreviations used in this article: 6A8, 6A8.6F10.1A6; APM, Ag-processing machinery; DC, dendritic cell; ES, effector silent; GAH, goat anti-human; GAM, goat anti-mouse; h, human; KO, knockout; β2m, β_2-microglobulin; m, mouse; Qdm, Qa-1 determinant modifier; RT, room temperature; SA, streptavidin; TCRL, TCR-like.

microenvironment. Additionally, because of the growing importance of the NKG2A immune checkpoint in cancer immunity, an Ab that selectively bound to the Qa-1^b/Qdm peptide complex and not to Qa-1^b independent of peptide loaded (24), could be used to explore the potential therapeutic effect of blocking the ligand side of the NKG2A axis.

To address these points, we generated a TCR-like (TCRL) or TCR-mimicking Ab to the Qa-1^b/Qdm complex. TCRL Abs have been made to many different HLA/peptide complexes (25–27); however, to the best of our knowledge, none exists to peptides presented by nonclassical MHC, including the Qa-1^b/Qdm complex. To this end, we constructed a single-domain Ab library for yeast surface display after immunizing a llama with recombinant Qa-1^b/Qdm protein. Screening of the single-domain Ab library for binders to Qa-1^b/Qdm yielded a unique clone, EXX-1. In this study, we characterize EXX-1 and show that this TCRL Ab staining of cancer cells is Qa-1^b–dependent and Qdm peptide specific and displays functional activity in vitro by disrupting the NKG2A/Qa-1^b axis to unleash NK cytolysis of tumor cells.

Materials and Methods

Library generation and yeast library construction

Immunization of a *Lama glama* with Qa-1^b/Qdm was performed by Capralogics as described previously (28) and followed by the construction of a phage display library by Creative BioLabs. (The immunization protocol was reviewed and approved by the IACUC committee at Capralogics, and all work was performed under veterinary oversight with strict adherence to standard operating procedures). To convert from a phage display library to a yeast display library, an appropriate amount of phagemid was used to cover at least 10-fold excess of the expected diversity. The VHH genes were amplified from phagemid using the forward primers Lla_04, Lla_05 and Lla_06 and the reverse primer Lla_07 (primer sequence shown in Table I). The primers were modified to allow for cloning into the yeast display vector. The yeast strain EBY100 (ATCC) was transformed with pYES3/Aga2 vector (modified from pYES3/CT, Thermo Fisher Scientific) containing cloned VHH genes according to the protocol of Van Deventer and Wittrup (29). Multiple electroporations were pooled, with 200 ng of vector and 2 μg of VHH used in each electroporation. Dilution plates indicated the number of transformants, and colony PCR was used to quantify inserted sequence quality.

Screening for binders to the Qa-1^b/Qdm complex

For staining and selection purposes, the VHH single-domain Ab library was incubated overnight in galactose-rich media at 30°C to induce expression of Ab molecules for display on the surface of yeast. Yeasts were resuspended in blocking buffer (5% BSA, 0.05% Tween 20 in PBS) for 30–60 min at room temperature (RT) with rotation. Yeasts were then incubated with biotinylated Ag (Qa-1^b/QDM, Qa-1^b/β_2m [β_2-microglobulin] not containing peptide [Qa-1^b no peptide], Qa-1^b/Q001, Qa-1^b/Q002, and Qa-1^b/DDX5) followed by incubation for 30–90 min at 4°C, with incubation time dependent on Ag concentration. Biochemical purification and tandem mass spectrometry was used previously to identify peptides Q001, Q002, and DDX5 that bind to Qa-1^b (9). Yeasts were washed with staining buffer (0.5% BSA, 0.05% Tween 20 in PBS) and resuspended in staining buffer containing anti-FLAG tag (DYKDDDDK) Ab conjugated with FITC and streptavidin (SA) conjugated to R-PE. After a 30-min incubation at 4°C, yeasts were washed three times and resuspended in staining buffer. Yeasts were analyzed on a Beckman Coulter CytoFLEX S. Data were analyzed using FlowJo software version 10. Yeasts were first gated based on forward scatter and side scatter to remove debris, followed by selection of singlets before analyzing Ag binding (PE) versus VHH expression (FITC). For MACS selection, after blocking, yeasts were resuspended in 0.5–1 ml of Qa-1^b/Qdm at 1 μM and incubated for 30 min at 4°C. After washing, yeasts were resuspended in 5 ml of staining buffer with 400 μl of SA microbeads (Miltenyi Biotec, catalog no. 130-048-101) for 20 min at 4°C. Yeasts were selected for binding to SA microbeads using LS columns (Miltenyi Biotec, catalog no. 130-042-401). MACS selection was performed once, followed by two rounds of sorting on a FACSAria II (BD Biosciences). For sorting, yeasts were stained as described above.

Mouse tumor cell lines and 293T.Qa1/Db transfectant

The tumor cell lines B16F10, B16F10 Qa-1^b knockout (Qa-1^{bKO}), TC-1, TC-1 Qa-1^{bKO}, RMA, and RMA Qa-1^{bKO} have been described previously (4). The C1498 cell line was purchased from Imanis Life Sciences. B16F10.D^b KO cells were described before (30). The 293T.Qa-1^b/D^b–transfected cell line was a gift from Dr. Peter Dyson. Briefly, the Qa-1^b/D^b chimera was constructed using the α3 segment and transmembrane and intracellular domains from the H2-D^b molecule and the α2 and α3 segments from Qa-1^b for these transfectants (31). All cells were cultured in recommended medium. Cell lines were authenticated and confirmed free of rodent viruses and *Mycoplasma* by routine testing by IDEXX.

Reagents and Abs for flow cytometry

Reagents SA-allophycocyanin (catalog no. 405204), Zombie Aqua fixable viability kit (catalog no. 423101/423102), calcein-AM (catalog no. 425201), TrueStain FcX plus (catalog no. 156604), and FluoroFix buffer (catalog no. 422101) and anti-mouse NKp46-BV421 (29A1.4; catalog no. 137612) were purchased from BioLegend. SA-PE (catalog no. 12-4317-87) was purchased from eBioscience. Anti–FLAG-AF488 (catalog no. IC8529G) and anti-mouse Fcγ RI/CD64 (catalog no. 290322) were purchased from R&D Systems. Anti-mouse NKG2A/C/E-PE (20d5; catalog no. 130-105-620) was purchased from Miltenyi Biotec, and H2-D^b-PE (28-14-8; catalog no. A15443) was from Thermo Fisher Scientific. Abs specific for anti-mouse CD3-BV421 (17A2; catalog no. 555276) and biotin-labeled anti-mouse Qa-1^b (6A8.6F10.1A6 [6A8]; catalog no. 559829) were purchased from BD Pharmingen. AffiniPure goat anti-human (GAH) IgG, Fcγ fragment specific (catalog no. 109-115-098) and AffiniPure goat anti-mouse (GAM) IgG (subclasses 1 + 2a + 2b + 3) (catalog no. 115-115-164), GAM-allophycocyanin (catalog no. 115-135-164), GAM-PE (catalog no. 115-115-164), GAH-allophycocyanin (catalog no. 109-135-098), and GAH-PE (catalog no. 1150098) were purchased from Jackson ImmunoResearch Laboratories. A CytoFLEX S V4-B2-Y4-R3 flow cytometer (Beckman Coulter) was used, and flow cytometry data were analyzed with FlowJo software version 10.

Peptides

Peptide Qdm (AMAPRTLLL) was synthesized by MBL International. Peptides D^k (AMVPRTLLL), K^b (MVPCTLLLL), Q001 (AQAERTPEL, DENN domain-containing protein 3), Q002 (IINTHTLLL, IQ motif containing GTPase activating protein 1), EPH (TLADFDPRV, erythropoietin-producing human hepatocellular receptor), DDX5 (ATPGRKDFL, DEAD box protein 5), glycine/alanine-substituted Qdm peptides (p1A→G, p3A→G, p4P→A, p5R→A, p6T→A, p7L→A, and p8L→A), and lysine-substituted Qdm peptides (Lys-P5 and Lys-P8) were synthesized by GenScript.

Production of Qa-1^b peptide monomers

The extracellular domain of mouse Qa-1^b containing a C terminus *BirA* peptide sequence for biotinylation and human β_2m genes were cloned in pET21(+) vector purchased from Sigma-Aldrich and transformed into BL21(DE3) *Escherichia coli* (New England Biolabs). Proteins were produced, purified from inclusion bodies, and used in refolding reactions with synthesized peptides to produce Qa-1^b/peptide complexes as described previously (12). The Qa-1^b/peptide mixture was concentrated, and the correctly folded complex was isolated from impurities using size-exclusion chromatography and a Superdex 75 column (GE Healthcare Biosciences). A portion of the purified refolded complex, designated as active monomer, was biotinylated using the *BirA* biotin ligase enzyme (Avidity) and purified a second time on the Superdex 75 column. Purified material (unbiotinylated and

Table I. Primers used for yeast display library construction

Primer	Sequence (5′→3′)
Lla_04	ATAGCTCGACGATTGAAGGTAGAGCGGCCGCTTACCCATACGACGTTCCAGACTACGCT**CAGGTGCAGCTGGTGCAGTCTGG**
Lla_05	ATAGCTCGACGATTGAAGGTAGAGCGGCCGCTTACCCATACGACGTTCCAGACTACGCT**CAGGTCACCTTGAAGGAGTCTGG**
Lla_06	ATAGCTCGACGATTGAAGGTAGAGCGGCCGCTTACCCATACGACGTTCCAGACTACGCT**CAGGTGCAGCTGCAGGAGTCGGG**
Lla_07	GATGCGGCCCTCTAGGATCAGCGGGTTTAAACTCACTTGTCGTCATCGTCTTTGTAGTC**TGAGGAGACRGTGACCTGGGTCC**

Bold font represents sequence complementary to the V gene segments.

biotinylated) was analyzed by mass spectrometry to detect Qa-1^b H chain, β_2m, peptide (indicating peptide loading), and the percentage of material that was biotinylated (for biotin-labeled molecules). All mass spectrometry work was performed at the Proteomics Core Lab at the UT Southwestern Medical Center.

Ab production

The expression tests in mammalian cells were performed in Expi293F cells (Thermo Fisher Scientific, catalog no. A14527). The VHH region of EXX-1 or its isotype control, anti-hCD3e VHH, was cloned into either human pFUSE-human (h)IgG1-Fc2 (catalog no. pfuse-hg1fc2) or mouse pFUSE-mouse (m)IgG2a-Fc2 (catalog no. pfuse-mg2afc2) vector purchased from InvivoGen. Cells were transfected transiently with expression vectors according to the manufacturer's instructions. At 5 d posttransfection, Ab-containing supernatants were harvested. The Abs were captured and purified using protein A beads (GenScript, catalog no. L00210.). After buffer exchange into PBS using Amicon ultra-4 centrifugal filters (EMD Millipore), Abs were analyzed for correct size and purity. SDS-PAGE was performed under either reducing or nonreducing conditions using Mini-PROTEAN TGX stain-free polyacrylamide gels and the Mini-PROTEAN tetra system purchased from Bio-Rad. SDS-PAGE gels were stained with Coomassie blue for visualization. Additional purified samples were run on an analytical-grade Superdex 200 column (GE Healthcare Biosciences) for size and purity determination. Larger scale production of EXX-1 mFc and associated controls and production of EXX-1 hFc (effector silent [ES]) and EXX-1 mFc (ES) and associated controls were done by ATUM.

ELISA

High protein–binding flat-bottom 96-well plates (Nunc MaxiSorp) were coated with 50 μl of NeutrAvidin (50 mg/ml in PBS) in each well and incubated overnight at 4°C. Plates were washed three times with wash/assay buffer (0.1% BSA, 0.05% Tween 20 in PBS). Available protein-binding sites were blocked with 100 μl/well blocking buffer (5% BSA, 0.05% Tween 20 in PBS) and incubated for 1 h at RT. Buffer was discarded, plates were washed three times in wash buffer, and 50 μl of biotinylated monomer (Qa-1^b/peptide complex) was diluted in wash/assay buffer with final concentrations of 5, 2.5, 1.25, and 0.625 μg/ml and incubated for 1 h at RT. Plates were washed four times with assay buffer (200 μl/well) and allowed to soak for 12 min before the addition of Abs. Abs were diluted in the assay buffer with the concentrations of 2.5, 1.25, and 0.625 μg/ml, and 50 μl of diluted Abs (anti-β_2m [Thermo Fisher Scientific, clone B2M-01, catalog no. MA1-19141] and anti-mouse Qa-1^b (BD Biosciences, clone 6A8, catalog no. 744390) (positive controls) and isotype control hFc (negative control) and EXX-1 hFc [both Abs were produced in-house]) was added to their designated wells and incubated for 1 h at RT. Plates were washed five times (200 μl/well) before adding anti-human HRP (catalog no. 109-035-088) or anti-mouse HRP conjugates (catalog no. 115-035-003, Jackson ImmunoResearch Laboratories) diluted 1:5000 in assay buffer to designated wells and allowed to incubate for 1 h at RT to detect bound Ab. The plate was washed five times (200 μl/well), and 50 μl of 1-Step ultra tetramethylbenzidine-ELISA substrate solution (BD Biosciences) was added into each well, incubated for 30 min at RT, followed by the addition of 50 μl of stop solution (1 M hydrochloric acid) and read at 450 nm on a Synergy 2 multi-mode microplate reader (BioTek Instruments).

Affinity and binding specificity determined using label-free bioassay system

The binding affinity of EXX-1 was determined using label-free technology (ResoSens instrument, Resonant Sensors). The dissociation equilibrium constant was determined as follows. Thermo Fisher Scientific CaptureSelect biotin anti-human IgG-Fc (catalog no. 7103262100, diluted in PBS buffer) was immobilized on NeutrAvidin-coated Bionetics label-free microarray plates at 5 μg/ml until binding reached equilibrium. The plate was subsequently washed three times with dilution/wash buffer (0.1% BSA, 0.05% Tween 20 in PBS). EXX-1 hFc (10 μg/ml in dilution/wash buffer) was captured by anti-human IgG-Fc until binding reached equilibrium. The plate was subsequently washed three times in dilution/wash buffer. The Qa-1^b/Qdm monomer complex (serial dilutions starting at 20 μg/ml in dilution/wash buffer) was added to wells and allowed to incubate for 20 min to determine the binding association. Then, excess Ag was removed, replaced with fresh wash buffer, and immediately incubated on a reader for ~25 min to determine the dissociation rate. Binding affinity was calculated using TraceDrawer kinetic analysis software.

Binding specificity was also determined by a ResoSens label-free bioassay system using Integrated ResoVu software, which was used for data acquisition and statistical analysis (Resonant Sensors).

Staining of tumor cells

When cultured target cells reached ~70–80% confluence, 20 ng/ml recombinant mIFN-γ (R&D System) was added to the cells and further incubated for 48 h at 37°C. Adherent cells were treated using trypsin-EDTA solution (MilliporeSigma), and recovered cells were washed three times with FACS buffer (PBS supplemented with 2% FBS [Life Technologies] and 2 mM EDTA [Invitrogen]). Then, 100,000–200,000 cells/well were used for staining.

Fc block (mouse TruStain FcX plus) was added to wells with cells and incubated for 15 min at 4°C before adding 50 μl of primary Ab and incubated for 30 min at 4°C. Cells were washed with the addition of 100–150 μl/well of FACS buffer before the addition of secondary Ab conjugates. GAH-Fc/PE or GAM-Fc/PE was added to wells at 1:100 dilution in FACS buffer. For detection of biotin-labeled Abs, SA-PE was added at a 1:50 dilution in FACS buffer. All samples were stained using Zombie Aqua viability stain and washed three times with FACS buffer. Cells were fixed by adding 100–200 μl/well FluoroFix buffer before analysis. For gating, cells were first selected based on forward scatter and side scatter, followed by selection of singlets and live cells. A CytoFLEX S V4-B2-Y4-R3 flow cytometer (Beckman Coulter) was used, and flow cytometry data were analyzed with FlowJo software version 10.

Cytotoxic assays with mouse NK cells

The effector cells used were NK cells enriched (EasySep mouse NK cell isolation kit, STEMCELL Technologies) from spleens of naive C57BL/6 mice (The Jackson Laboratory), with a purity >90%. NK cells were incubated at 1×10^6/ml with recombinant mIL-2 (20 ng/ml) for 24 h. NK cells were cocultured at a ratio of 3:1 with target cell lines, B16 Qa-1^{b+} or B16 Qa-1^{bKO}, that had been previously incubated with mIFN-γ for 48 h and that were labeled with calcein-AM. Abs were added at 10 μg/ml. Plates were incubated for 24 h at 37°C and read at 490 nm on a Synergy 2 multi-mode microplate reader (BioTek Instruments). Cell lysis was calculated according to the formula: [(test release − spontaneous release)/(maximum release − spontaneous release)] × 100. Spontaneous release represents calcein-AM release from untreated target cells, and maximum release represents calcein-AM release from target cells lysed with 2% Triton X-100 (MilliporeSigma).

Statistical analysis

Statistical analyses were performed using GraphPad Prism software (GraphPad Software, San Diego, CA). The data are expressed as the mean ± SD and were analyzed with one-way ANOVA followed by a Dunnett or Tukey post hoc test.

Results

Identification of anti–Qa-1^b/Qdm TCRL Ab EXX-1

To generate TCRL Abs with specificity for Qa-1^b/Qdm, a llama was first immunized with complexes of recombinant Qa-1^b/Qdm following the protocol described previously (28). One week after the final immunization, blood was collected, B cells were enriched, mRNA was isolated, and VHH genes were amplified and cloned into phagemid vector. A second round of VHH gene amplification was performed using phagemid with VHH sequences, and forward primers and a reverse primer shown in Table I were used to construct the yeast display library and screen for binders. MACS selection was done (R1 out) using target Ag (Qa-1^b/Qdm) at 1 μM. The R1 library was checked for binders recognizing the target, and a substantial enrichment was observed in the number of binders recognizing the Qa-1^b/Qdm complex compared with controls; that is, Qa-1^b no peptide and Qa-1^b loaded with one of the following control peptides: Q001, Q002, and DDX5. Peptides Q001, Q002, and DDX5 were shown previously to bind to Qa-1^b (9). To select for binders with enhanced affinity through selective gating, the R1 library was sorted using FACS (R2 out). This was repeated a final time for a total of three selections (R3 out). The R3 library was then analyzed for unique binders specific for Qa-1^b/Qdm. In total, five unique binders were found and tested for specificity using the panel

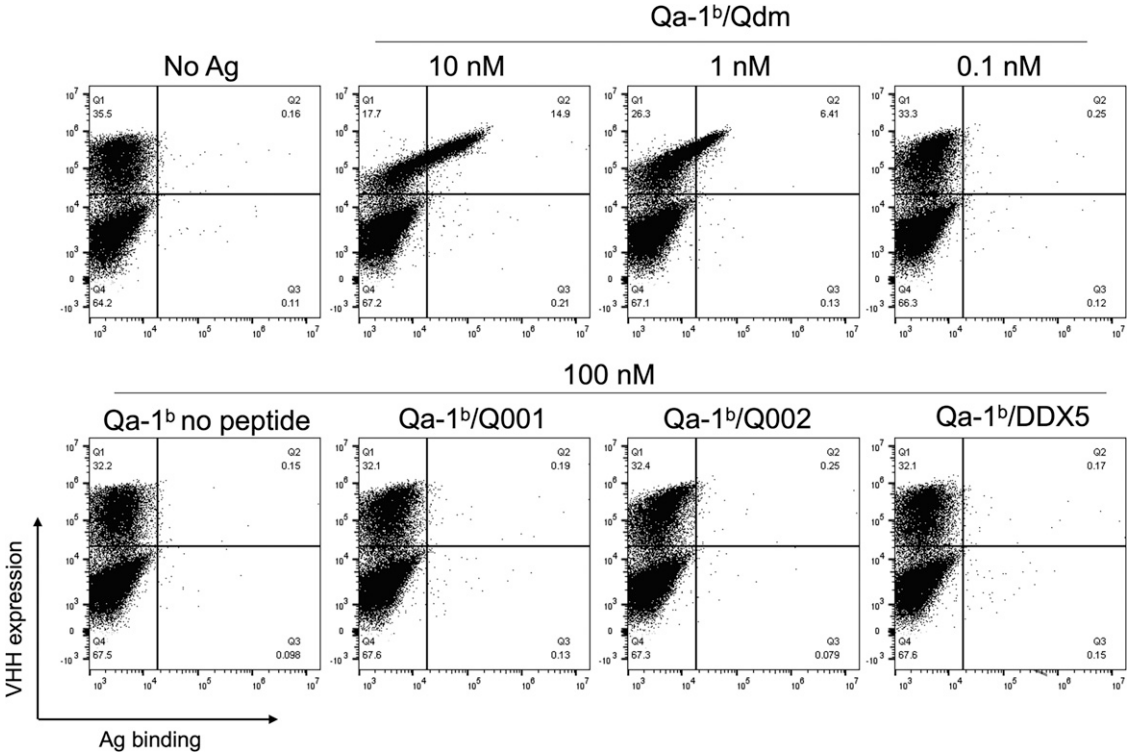

FIGURE 1. Yeast display of clone EXX-1. Staining of the single clone EXX-1 in yeast. Ag binding is indicated in Q2, with staining for both VHH expression and Ag binding. VHH expression was detected with an anti-FLAG epitope tag. Ag binding of biotinylated Ags was detected with SA-PE. Histograms plotted are representative of at least two independent staining experiments.

of control peptides loaded into Qa-1^b. One clone, termed EXX-1, showed the best combination of binding sensitivity (1 nM Ag) and specificity for Qa-1^b/Qdm (Fig. 1).

Characterization of the top clone, EXX-1

EXX-1 was cloned into the pFUSE-IgG-Fc expression vector containing either human IgG1 (hFc), human IgG1 with mutations at Leu234Ala and at Leu235Ala (LALA mutations; hFc ES), mIgG2a (mFc), or mIgG2a with LALA mutations (mFc ES) and produced in Chinese hamster ovary (CHO) cells or Expi293 cells using a transient transfection protocol followed by purification by protein A affinity chromatography. LALA mutations were introduced to reduce nonspecific binding to Fcγ receptors and the Fc domain of human and mouse IgGs. An example of sample purity was shown for the EXX-1 mFc molecule by SDS-PAGE under reduced (a single band at 41 kDa representing monomer VHH-IgG) and nonreduced conditions (single band at ~90 kDa) (Fig. 2A) and by observing a single peak by size-exclusion chromatography (Fig. 2B). The binding affinity of EXX-1 hFc was determined with a dissociation equilibrium constant of 1.73 nM.

EXX-1 specifically recognizes the Qa-1^b/Qdm complex

We next evaluated by ELISA the binding specificity of the EXX-1 hFc to recombinant mQa-1^b loaded with specific peptide Qdm, control peptide Q001, or Qa-1^b no peptide. EXX-1 hFc was immobilized in wells at 0.25 μg/ml, and binding to Qa-1^b monomer samples was evaluated at various concentrations (0.125, 0.062, and 0.031 μg/ml) and shown to be selective for the Qa-1^b/Qdm complex in a dose-dependent manner (Fig. 2C). In contrast, EXX-1 hFc displayed little to no binding to control Ags, Qa-1^b/Q001 and Qa-1^b no peptide. Anti-β_2m Ab bound to Qa-1^b/Qdm, Qa-1^b/Q001, and Qa-1^b empty, indicating the presence of β_2m associated with Qa-1^b. In addition, anti–Qa-1^b Ab (clone 6A8) demonstrated the presence of the Qa-1^b H chain in all complexes (Fig. 2C). Next, we assessed by ELISA the detection sensitivity of EXX-1 hFc. Plates were coated with Qa-1^b/Qdm, Qa-1^b/Q001, or Qa-1^b no peptide starting at 0.25 μg/ml with 2-fold serial dilutions down to 0.0312 μg/ml. EXX-1 hFc added to wells at 1 μg/ml showed detection of the Qa-1^b/Qdm complex, titrating down to background signal (~0.1 $OD_{450\ nm}$) at 0.0312 μg/ml. Only background signal was detected for EXX-1 hFc binding to controls, Qa-1^b/Q001 and Qa-1^b no peptide, supporting the specificity of EXX-1 binding for the Qa-1^b/Qdm peptide complex (Fig. 2D). Additionally, clone 6A8 and anti-β_2m Ab demonstrated the presence of the Qa-1^b H chain and β_2m, respectively. The isotype control Ab, a VHH single domain specific for hCD3ε containing hFc, did not bind to Qa-1^b/Qdm or control Qa-1^b molecules, as anticipated. Taken together, our findings demonstrate that EXX-1 Ab binding is highly specific even at low Ag concentrations for the Qa-1^b/Qdm peptide complex.

We next replaced the hFc domain of the EXX-1 Ab with an mFc (ES) domain to characterize its binding specificity in flow cytometry assays using human 293T cells. As expected, the binding specificity of EXX-1 mFc (ES) was unaltered after isotype switching (Fig. 2E).

Human 293T cells were previously transfected with Qa-1^b/D^b encoding plasmid (293T.Qa-1^b/D^b) cells and were either not pulsed (unpulsed) or pulsed with 1 μM peptides (Qdm, D^k, K^b, and Q001). The leader sequence peptide from D^k, AMVPRTLLL, was shown previously to bind to Qa-1^b (31). EPH peptide served as a negative control. Peptides were incubated with cells for 3 h at 37°C before staining with anti–Qa-1^b-biotin (clone 6A8) plus SA-PE or SA-PE alone (control) or EXX-1 mFc (ES) plus GAM-PE conjugate or GAM-PE conjugate alone (control). 293T.Qa-1^b/D^b cells stained with the clone 6A8 Ab (Fig. 3A, top panel) show staining of 293T.Qa-1^b/D^b cells before and after pulsing with peptides Qdm, D^k, K^b, Q001, or EPH, indicating Qa-1^b expression. In contrast, the EXX-1 mFc (ES) Ab only stained 293T.Qa-1^b/D^b cells following pulsing with the Qdm peptide, as shown in Fig. 3a, bottom panel, and 3C). A notable finding was

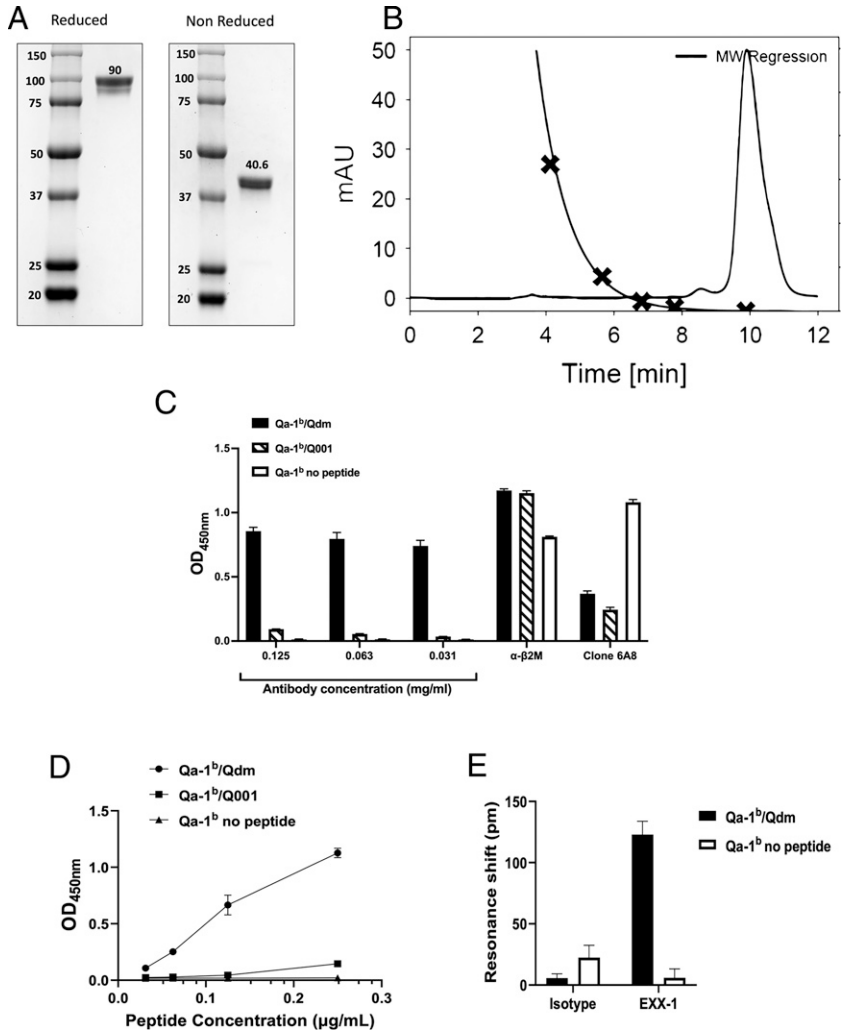

FIGURE 2. EXX-1 binds to recombinant Qa-1^b/Qdm complexes. (**A** and **B**) Characterization of purified EXX-1 hFc by (A) SDS-PAGE under reduced and non-reduced conditions and (B) by size exclusion chromatography. (**C**) Assessment of EXX-1 hFc specificity by ELISA. Plates were coated with EXX-1 hFc (0.125, 0.062, and 0.03201 μg), anti-β_2m (0.5 μg), or anti–Qa-1^b (clone 6A8, 0.5μg). Complexes of biotinylated Qa-1^b monomers (Qa-1^b/Qdm, Qa-1^b/Q001, or Qa-1b no peptide) were added at 0.25 μg/ml. (**D**) Assessment of EXX-1 (1 μg/ml) detection sensitivity by ELISA to Qa-1^b complexes (Qdm, Q001, no peptide) immobilized at 0.25, 0.125, 0.0625, and 0.0312 μg/well. (**E**) Assessment of EXX-1 mFc (ES) (1 μg/ml) binding to immobilized Qa-1^b/Qdm or Qa-1^b no peptide using the ResoSens label-free bioassay system. In (C)–(E), error bars represent mean ± SEM of triplicate samples and are representative of three independent experiments.

that EXX-1 did not bind to 293T.Qa-1^b/D^b cells pulsed with the leader sequence peptide from MHC D^k, having only a single amino acid difference at position 3 from the Qdm peptide. To assess Qa-1^b expression, 293T.Qa-1^b/D^b cells were stained with clone 6A8 and all cells, unpulsed and peptide pulsed, showed similar levels of Qa-1^b expression (Fig. 3B). Importantly, only cells pulsed with Qdm peptide were stained with EXX-1 mFc (ES) Ab (Fig. 3C), demonstrating that control peptides bound to Qa-1^b were not recognized by EXX-1 Ab. To expand our investigation into the binding selectivity of EXX-1, 293T.Qa-1^b/D^b cells were pulsed with different concentrations of peptides Qdm, Q001, and Q002 and then stained with EXX-1 mFc (ES) prior to assessing by flow cytometry. EXX-1 mFc (ES) exhibited dose-dependent binding to 293T.Qa-1^b/D^b cells pulsed with Qdm peptide at all concentrations (5.0–0.0097 μM) with only background staining to cells pulsed with peptides Q001 and Q002 (Fig. 3D). These results indicate that EXX-1 Ab retains binding selectivity even in the presence of low target density and that EXX-1 binding to Qdm peptide is dependent, in part, on making contact with the p3 alanine residue.

IFN-γ is required for EXX-1 binding to mouse tumor cell lines in vitro

Next, clone 6A8 and EXX-1 Ab were used to stain several in vitro–cultured murine tumor cell lines, that is, TC1 (carcinoma), B16 (melanoma), RMA (leukemia), and C1498 (leukemia), for expression of Qa-1^b and Qa-1^b/Qdm complex, respectively. The results, shown in Fig. 4A and 4B, clearly demonstrate a lack of EXX-1 mFc (ES) Ab staining in the absence of recombinant mIFN-γ, indicating that these mouse tumor cell lines do not constitutively express the Qa-1^b/Qdm complex. This was not unexpected, as it was previously reported by van Montfoort et al. (4) that exposure of cells to mIFN-γ was needed to induce expression of Qa-1^b on tumor cells in vitro. Furthermore, mIFN-γ–stimulated tumor cells were all stained by both clone 6A8 and EXX-1 Ab, indicating that stimulation with IFN-γ not only upregulated cell surface expression of Qa-1^b molecules but induced expression of the Qa-1^b/Qdm complex.

We next treated the Qa-1^b knockdown variants (Qa-1^{bKO}) of TC1, B16, and RMA with mIFN-γ before flow cytometric analysis. Results shown in Fig. 4C reveal that mIFN-γ did not induce Qa-1^b expression in Qa-1^{bKO} tumor cells. These findings further support the role of IFN-γ in regulating the expression of the Qa-1^b/Qdm complex (Fig. 4). Collectively, these data show that EXX-1 binding is Qa-1^b–dependent and that Qa-1^b/Qdm complex expression in tumor cells in vitro is induced by IFN-γ.

EXX-1 mFc (ES) binding is specific for the Qdm peptide presented by Qa-1^b

To provide additional evidence of Qdm peptide specificity for EXX-1, murine tumor cell lines B16F10 (wild-type) and B16F10.D^{bKO} (MHC D^b gene KO) were treated overnight with mIFN-γ and stained with either anti-D^b, clone 6A8, or EXX-1 Abs. B16F10 tumor cells were shown to express high levels of MHC class Ia D^b, but genetic KO of

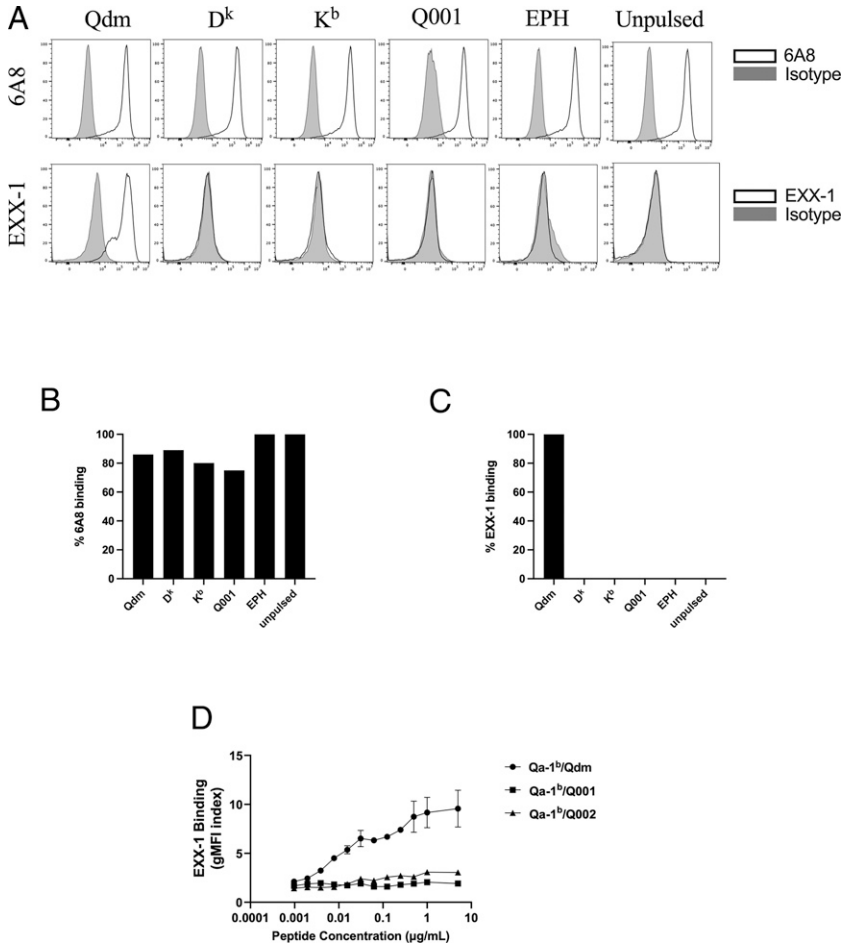

FIGURE 3. EXX-1 Ab recognizes Qdm on peptide-pulsed 293T.Qa-1^b/D^b cells. Qa-1^b–transfected 293T cells (293T.Qa-1^b/D^b) were left unpulsed or pulsed for 3 h at 37°C with 1 μM of the following peptides: Qdm, Q001, D^k, K^b, or EPH as indicated. (**A**) Unpulsed 293T.Qa-1^b/D^b and peptide-pulsed 293T.Qa-1^b/D^b cells were stained with (top panel) 1 μg/ml of clone 6A8-biotin (1° Ab) and SA-PE (2° Ab) or (bottom panel) 1 μg/ml EXX-1 hFc (1° Ab) and GAH-PE (2° Ab). Filled gray denotes isotype and black solid line denotes staining with indicated Ab. (**B**) Percent binding of clone 6A8 to unpulsed 293T.Qa-1^b/D^b cells or 293T.Qa-1^b/D^b cells pulsed with 1 μM peptide. Cells pulsed with Qdm and EPH peptides serve as positive and negative controls, respectively. Note that efficiency of peptide loading of 293T.Qa-1^b/D^b cells is reflected by a percent decrease in clone 6A8 binding compared with EPH peptide-pulsed and unpulsed cells (100%). (**C**) EXX-1 Ab only binds to Qdm-pulsed 293T.Qa-1^b/D^b. In (A)–(C), mean fluorescence intensity (MFI) = [(MFI of cells stained with 1° Ab + 2° Ab) − (MFI of cells stained only with 2° Ab)], and results are representative of at least three independent experiments. (**D**) 293T.Qa-1^b/D^b cells were pulsed with a titration (5–0.00097 μM) of peptides (Qdm, Q001, or Q002) and stained with EXX-1 hFc at 1 μg/ml. Geometric MFI (gMFI) index = [(gMFI of cells stained with 1° Ab + 2° Ab) ÷ (gMFI of cells stained only with 2° Ab)]. In (A)–(C), staining results are representative of at least three independent experiments. In (D), error bars represent mean ± SEM of triplicates samples and are representative of at least three independent experiments.

this gene indeed led to absence of the D^b protein (Fig. 5). Because H-2D^b is the only classical MHC molecule delivering the Qdm in C57BL/6 cells, B16F10.D^{bKO} cells are deficient for Qdm peptide and therefore lack presentation of the Qa-1^b/Qdm complex (32). Importantly, the B16F10.D^{bKO} cells were not stained with EXX-1, although staining was still observed with clone 6A8. Taken together, these data demonstrate that EXX-1 specifically recognizes Qdm peptide in Qa-1^b and further suggest that B16F10.D^{bKO} cells may express the Qa-1^b H chain alone or potentially Qa-1^b with peptides other than Qdm.

Alanine scan analysis to determine EXX-1 interaction with residues of Qdm peptide

To determine which residues of Qdm peptide are critical for EXX-1 interaction, seven mutated forms of the peptide were synthesized. Each variant contained a single residue substitution with either alanine or glycine (G1, G3, A4, A5, A6, A7, and A8) and was used to pulse 293T.Qa-1^b/D^b cells expressing the peptide-binding groove of Qa-1^b. Peptides with alanine mutations in residues p2 and p9 were not used because these are primary anchor residues for Qdm peptide binding to Qa-1^b (33). All 293T.Qa-1^b/D^b cells pulsed with these different peptides stained similar with clone 6A8, indicating comparable surface display of peptide/Qa-1^b complexes (Fig. 6A). In contrast, EXX-1 staining of peptide-pulsed 293T.Qa-1^b/D^b cells revealed a marked reduction (≥95%; $p < 0.0001$) in staining signal when cells were pulsed with variant peptides G3, A6, A7, or A8 compared with wild-type Qdm peptide (Fig. 6B). Additionally, a more modest reduction of 20% to ~60% was observed for EXX-1 staining signal when 293T.Qa-1^b/D^b cells were pulsed with peptides A4 or A5 compared with wild-type Qdm peptide (Fig. 6B). We conclude from these studies that EXX-1 Ab has multiple interactions across the Qdm peptide, making crucial contact with residues p3, p6, p7, and p8.

To further attempt mapping of EXX-1 Ab interaction with the nonanchor position P8 in Qdm peptide, leucine, a hydrophobic amino acid, was substituted with lysine (P8 L-K), an amino acid with a basic side chain, and used to pulse 293T.Qa-1^b/D^b cells. Additionally, the nonanchor position P5 containing an arginine residue in Qdm peptide was substituted with lysine (P5 R-K), a less bulky amino acid with a basic side chain, and used as a control for loading in Qa-1^b and for binding to EXX-1. Previously, Kraft et al. (33) had shown that lysine substitutions in Qdm peptide at positions 5 or 8 produced only small effects on peptide binding to Qa-1^b. To confirm that these lysine substituted peptides were loaded in Qa-1^b, 293T.Qa-1^b/D^b cells were pulsed with peptides (wild-type Qdm, P5 R-K, or P8 L-K) and stained with clone 6A8. As shown in Fig. 6C, clone 6A8 bound to all cells. Next, unpulsed and peptide-pulsed 293T.Qa-1^b/D^b cells were stained with EXX-1 Ab (Fig. 6D). As expected, EXX-1 binding to unpulsed cells was not detected. In contrast, EXX-1 binding was modestly reduced (~20%) to cells pulsed with the P5 R-K peptide, suggesting that EXX-1 Ab had only minor interaction with the P5 residue. When cells pulsed with P8 L-K peptide were stained with EXX-1 Ab, a reduction of binding signal (>60%) was observed compared with wild-type Qdm peptide-pulsed cells, indicating EXX-1 contact with leucine at P8, although this interaction was not found to be critical for EXX-1 binding. Taken together, our findings suggest that EXX-1 makes primary contact with wild-type Qdm peptide residues P3, P6, P7, and P8 and additional though noncritical contact with residues P4 and P5, reinforcing the notion that EXX-1 binding is selective for the Qdm peptide in Qa-1^b.

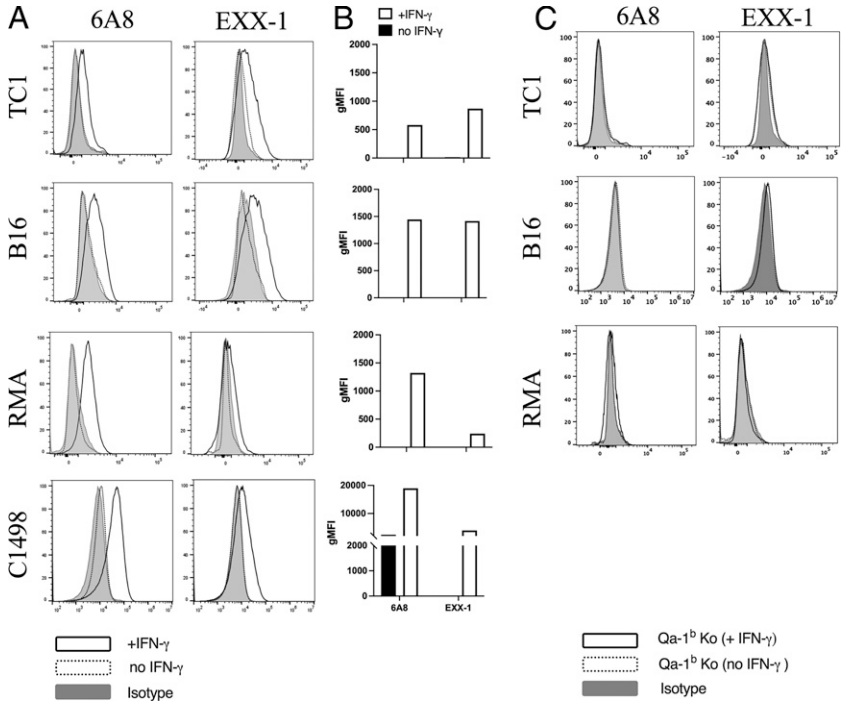

FIGURE 4. Assessment of EXX-1 binding to mouse tumor cells in vitro. (**A**) Clone 6A8 (left panel) and EXX-1 (right panel) with (**B**) summarized data for TC-1, B16, RMA, and C1498 cells. Cells were stimulated with recombinant mIFN-γ (20 ng/ml) for 48 h prior to staining with Abs. (**C**) Clone 6A8 (left panel) and EXX-1 (right panel) were used to stain TC1, B16, and RMA Qa-1^{bKO} cells not stimulated or stimulated with recombinant mIFN-γ (20 ng/ml) for 48 h before staining with Abs. Geometric mean fluorescence intensity (gMFI) = [(gMFI of cells stained with 1° Ab + 2° Ab) − (gMFI of cells stained only with 2° Ab)]. In (A) and (C), filled gray represents isotype, dashed black line represents unstimulated, and solid black line represents staining of IFN-γ–stimulated cells. Samples were run in duplicate, and histograms shown are representative of at least three independent staining experiments.

Blockade of the NKG2A/Qa-1^b axis using EXX-1 Ab unleashes NK cell–mediated lysis of tumor cells in vitro

Having established that EXX-1 binding was specific for the Qa-1^b/Qdm complex, we attempted to determine whether EXX-1 could unleash NK cell lysis of B16 tumor cells by disrupting the NKG2A/Qa-1^b axis. Enriched mouse NK cells cultured in the presence of recombinant mIL-2 for 24 h were tested for cytolytic activity using mIFN-γ–stimulated B16 Qa-1^{b+} or B16 Qa-1^{bKO} cells as targets. As shown in Fig. 7, NK cells with PBS control displayed significantly greater killing (>30%) of B16 Qa-1^{bKO} cells compared with B16 Qa-1^{b+} cells, exhibiting the inhibitory power of Qa-1^b. When NK cells were treated with blocking NKG2A Ab, target cell lysis was restored to the level of Qa-1^b KO B16F10 cells. Importantly, EXX-1 mFc (ES) showed identical improvement in tumor cell killing (~30%) as compared with NKG2A blockade. Because EXX-1 mFc (ES) was an Fc-inert variant, killing was not FcR mediated but rather the result of disrupting the NKG2A axis. Furthermore, the isotype control for EXX-1 mFc (ES) did not restore target cell lysis. Collectively, these findings indicate that EXX-1 is effective at enhancing NK cell cytolytic activity by blocking the NKGA2/Qa-1^b axis.

Discussion

In this study we describe a novel research tool, a single-domain TCRL Ab for investigating the Qa-1^b/Qdm complex. The Ab, EXX-1, was characterized for binding affinity, specificity, and blocking activity in vitro. EXX-1 Ab binding selectivity was demonstrated using several methods, including genetic KO approaches and alanine scanning analysis. EXX-1 stained IFN-γ–treated wild-type

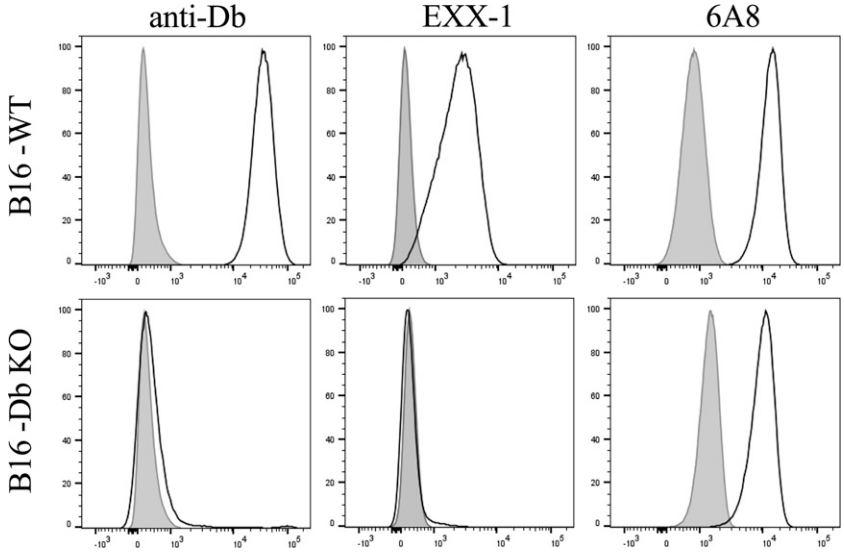

FIGURE 5. EXX-1 binding is selective for Qdm peptide in Qa-1^b. Staining with anti-D^b, EXX-1, or clone 6A8 in B16F10 wild-type (top panel) or B16F10.Db KO cells (bottom panel). Control reagent is plotted in gray. Indicated Ab is plotted with a black line. Cells were pretreated with IFN-γ for 24 h before staining with Abs. Histograms plotted are representative of at least two independent experiments.

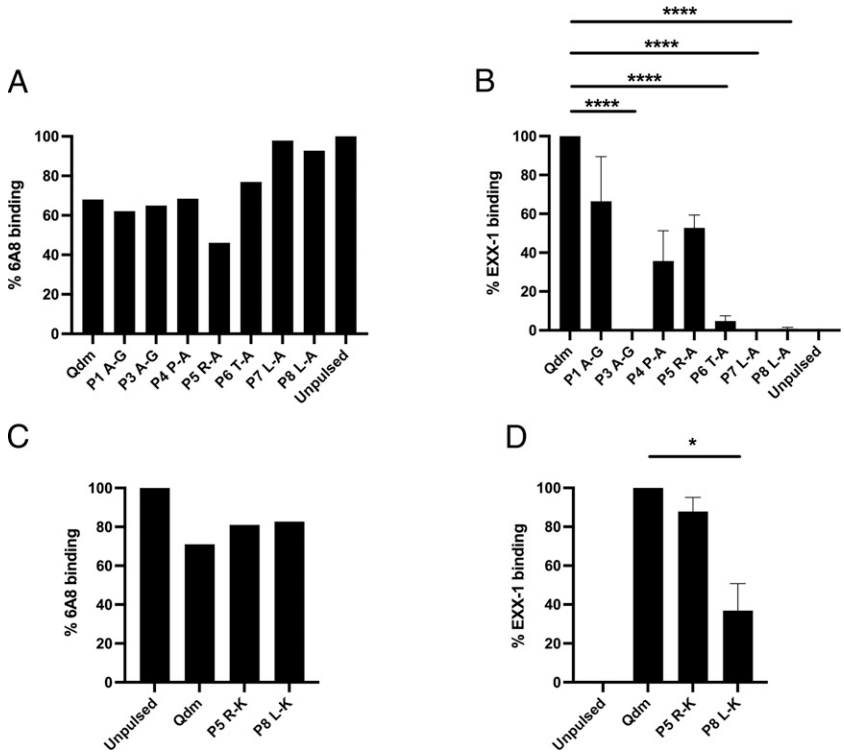

FIGURE 6. Alanine scan analysis reveals EXX-1 interactions with the Qdm peptide. (**A** and **B**) 293T.Qa-1^b/D^b cells were stained with 1 μg/ml clone 6A8 (A) or EXX-1 mFc (ES) (B) without peptide (unpulsed) or with 10 μg/ml wild-type Qdm or Qdm-variant peptides (p1A→G, p3A→G, p4P→A, p5R→A, p6T→A, p7L→A, p8L→A) as indicated. (**C** and **D**) 293T.Qa-1^b/D^b cells were stained with 1 μg/ml clone 6A8 (C) or EXX-1 (D) without peptide (unpulsed), wild-type Qdm, or variant Qdm peptides with lysine substitution at p5 R→K or p8 L→K as indicated. Clone 6A8-biotin binding was detected with SA-PE (2° Ab), and EXX-1 binding was detected with GAM-PE (2° Ab). Percent of binding for clone 6A8 to cells is calculated as [(MFI of clone 6A8 for cells pulsed with the indicated peptide) ÷ (MFI of clone 6A8 with unpulsed cells) × 100]. Percent of binding for EXX-1 to cells is calculated as [(MFI of EXX-1 in cells unpulsed or pulsed with the indicated peptide) ÷ (MFI of EXX-1 with Qdm) × 100]. Data shown in (A) and (C) are representative of two independent experiments. In (B) and (D), error bars represent mean ± SD from three independent studies. The p values were determined using one-way ANOVA followed by a Dunnett post hoc test. *$p < 0.01$, ****$p < 0.0001$.

B16, TC-1, and RMA tumor cells; conversely, IFN-γ–treated B16, TC-1, and RMA cells lacking Qa-1^b and B16 cells lacking D^b, which is the exclusive source of Qdm peptide, were not stained, demonstrating that EXX-1 is Qa-1^b–dependent and Qdm peptide specific, respectively. Furthermore, an additional murine tumor cell line, C1498, was stained with EXX-1 but only after overnight incubation with IFN-γ, suggesting that Qa-1^b/Qdm expression is tightly regulated by IFN-γ in tumor cells. Results from alanine scanning analysis showed that EXX-1 has critical interactions with several residues of the Qdm peptide. Moreover, when the EXX-1 Ab with an inactive mFc was evaluated in cytotoxicity assays, it was found to be effective at blocking the NKG2A/Qa-1^b inhibitory axis and promoting NK cytolysis of tumor cells in vitro.

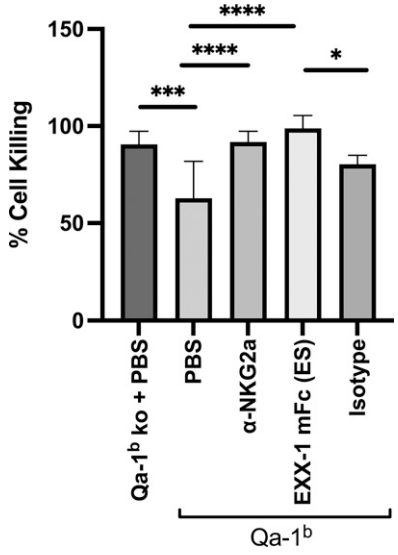

FIGURE 7. EXX-1 enhances NK cell cytolytic activity in vitro. Enriched NK cells isolated from spleens of naive C57BL/6 mice were incubated with recombinant mIL-2 (20 ng/ml) for 24 h. NK cells were then cocultured with mIFN-γ–stimulated and calcein-AM–labeled B16 Qa-1^{b+} or B16 Qa-1^{bKO} tumor cells at a ratio of 3:1 (E:T) with or without Abs as indicated for 24 h. Percent cell killing was assessed by measuring calcein-AM release. Error bars represent mean ± SD from three independent studies. The p values were determined using one-way ANOVA followed by a Tukey post hoc test. *$p < 0.01$, ***$p < 0.001$, ****$p < 0.0001$.

Multiple reports, including those from our laboratory, have described TCRL Abs and their use as novel research tools (26, 34–37). TCRL Abs are generally endowed with high affinity and target selectivity and because of this have been widely used to detect in real time specific peptide-loaded MHCs on the cell surface, helping to further our understanding of Ag presentation and regulation of peptide-loaded MHC expression (35, 38, 39). Although previous reports have described single-domain TCR-like Abs (40, 41), to the best of our knowledge the EXX-1 Ab is the first TCRL Ab identified that displays specificity for the Qdm peptide presented by Qa-1^b. A major challenge of TCRL Abs is their tendency to exhibit binding modes focused toward hotspots on the HLA surface that can lead to a greater degree of cross-reactivity (42). Interestingly, our attempts to find binders from either immunized or naive mouse libraries were unsuccessful in that the binders identified exhibited cross-reactivity, indicating a binding mode biased toward hotspots in the Qa-1^b molecule. To overcome this potential limitation, we constructed a single-domain VHH library and screened for binders having broad interactions across the peptide. VHH single-domain Abs have the smallest Ag-binding domain among Abs and can have a unique convex paratope architecture that prefers to associate with concave surfaces of the Ag compared with conventional Abs (43). The EXX-1 Ab identified using yeast surface display revealed p3, p6, p7, and p8 as primary contact residues. Our findings were further supported by determining Qa-1^b expression levels on peptide-pulsed cells using clone 6A8 (24). We observed comparable staining intensity with clone 6A8 to 293T.Qa-1^b/D^b cells presenting wild-type Qdm and Qdm-variant peptides. This suggests similar levels of Qa-1^b protein expression on the surface of all 293T.Qa-1^b/D^b cells, unpulsed and peptide pulsed, after staining with clone 6A8. Importantly, our data show that EXX-1 provides a uniquely selective

research tool for pursuing studies into the biology and function of the Qa-1^b/Qdm complex in healthy and diseased cells.

Early studies performed by the laboratories of Drs. J. Forman, M.J. Soloski, and others dissected the dominant presence of Qdm peptide (AMAPRTLLL) in Qa-1^b in mouse tumor cells using alloreactive CTL clones specific for Qa-1^b/Qdm complex and mass spectrometry (7, 44). These same groups observed that cells deficient in APM such as deletion of TAP1 were not lysed (44). These findings provided the initial support for Qdm being the dominant peptide loaded in Qa-1^b in cells having intact APM expressing MHC class Ia Ags, H2-D. Many studies since then have shown that the Qa-1^b/Qdm peptide complex is the ligand for the inhibitory heterodimeric receptor NKG2A/CD94, which is expressed on NK cells and tumor-infiltrating CD8$^+$ T cells (17). Moreover, expression of the Qa-1^b/Qdm complex on healthy cells has been postulated as a means to prevent lysis by NKG2A$^+$ NK cells (21). Support for this comes from several studies that showed normal dendritic cells (DCs) were protected from NK cell lysis but only after stimulation with CpG oligonucleotides or IFN-γ (20, 21). On the contrary, they found that unstimulated DCs were not protected from NK cell lysis (20, 21). Whether the lack of protection from NK lysis for unstimulated DCs was due to an absence of cell surface expression of Qa-1^b/Qdm complex expression is not known. However, our findings in the present study suggest that at least for some diseased cells, such as C1498 leukemia cells, there is a lack of Qa-1^b/Qdm complex expression in the absence of cytokine stimulation. Furthermore, a recent study performed by our laboratory found Qa-1^b molecule expression in resting C57BL/6 splenocytes after staining with clone 6A8; conversely, EXX-1 staining was not observed, suggesting that under homeostatic conditions Qdm peptide may not be available for presentation by Qa-1^b. An alternative explanation could be that Qa-1^b/Qdm complex density was below the detection threshold of EXX-1. Nonetheless, our findings raise questions regarding the regulation of Qa-1^b/Qdm expression in healthy cells and tissues and its postulated role in protecting cells against lysis from NK cells or CD8$^+$ T cells.

The fine binding selectivity of EXX-1 Ab will be useful for determining Qa-1^b/Qdm complex expression and its regulation during inflammation, infection, and cancer. It has been previously described that Qa-1^b is upregulated by cells and tissues under inflammatory conditions (45). Additionally, it has been shown that Qa-1^b expression can be increased during viral infection, likely regulated by proinflammatory cytokines such as IFN-γ and IFN-α (46, 47). In fact, Zhou et al. (48) showed that Qa-1^{bKO} mice infected with influenza were able to respond to the virus but were not able to effectively terminate the CD8$^+$ T cell response leading to immunopathology. This study and others suggest that Qa-1^b/Qdm is upregulated during stress or inflammatory conditions to downregulate the effector immune response mediated by CD8$^+$ T cells and NK cells to protect uninfected cells from unwanted lysis. Recently it has been demonstrated that the regulation of Qa-1^b expression in tumor cells is IFN-γ–dependent (4). However, in that study, it was not known whether Qa-1^b/Qdm complexes were being expressed. In our study, we observed EXX-1 binding to all mouse tumor cells evaluated but only after overnight incubation with mIFN-γ, suggesting that this cytokine has an important role in regulating Qa-1^b/Qdm complex expression. It also raises questions regarding Qa-1^b/Qdm regulation by IFN-γ and perhaps other cytokines in the tumor microenvironment. To this end, EXX-1 Ab may prove to be an invaluable tool for detecting and quantifying Qa-1^b/Qdm complexes and for elucidation of regulatory pathways controlling its expression in tumor tissue.

An exciting translational application for the EXX-1 Ab will be to explore its potential as a checkpoint blocking Ab. Several recent studies have shown that in tumor mouse models the expression of NKG2A is associated with worse clinical outcome (3, 4). For example, van Montfoort et al. (4) showed improved antitumor effects using B16, TC-1, and RMA tumor models by combining cancer vaccines with a mAb to the NKG2A receptor. André et al. (3) reported that Ab blockade of mouse or hNKG2A combined with anti–PD-L1 promotes antitumor immunity by unleashing both T and NK cell effector functions in vivo as well as in vitro. We show here that EXX-1 mFc (ES) can disrupt the NKG2A/Qa-1^b axis in vitro by binding to the Qa-1^b/Qdm complex to enhance NK cell–mediated killing of target cells. Our findings support further evaluation of EXX-1 as an immune checkpoint blocking Ab in tumor models. If healthy tissues do not express the Qa-1^b/Qdm complex but tumors do, especially in the presence of IFN-γ, as our findings suggest, targeting the Qa-1^b/Qdm complex with EXX-1 Ab might be useful as an immunotherapy approach. One potential caveat to targeting the Qa-1^b/Qdm peptide complex is that these molecules also serve as ligands for the related activating receptor, NKG2C. We would anticipate that EXX-1 Ab binding would interfere with NKG2C receptor binding to the Qa-1^b/Qdm complex, as both NKG2A and NKG2C form heterodimeric receptors with CD94 and have been shown to interact with the Qa-1^b/Qdm complex (49, 50). Future studies will be aimed at determining whether our novel Ab reagent blocks both NKG2A and NKG2C or only the NKG2A receptor. Nevertheless, it remains to be seen whether targeting tumor cells with TCRL Abs to the Qa-1^b/Qdm complex can effectively disrupt the NKG2A axis in vivo.

Disclosures

J.W. is a cofounder and chief scientist at Abexxa Biologics. The other authors have no financial conflicts of interest.

References

1. Borst, L., S. H. van der Burg, and T. van Hall. 2020. The NKG2A-HLA-E axis as a novel checkpoint in the tumor microenvironment. *Clin. Cancer Res.* 26: 5549–5556.
2. van Hall, T., P. André, A. Horowitz, D. F. Ruan, L. Borst, R. Zerbib, E. Narni-Mancinelli, S. H. van der Burg, and E. Vivier. 2019. Monalizumab: inhibiting the novel immune checkpoint NKG2A. *J. Immunother. Cancer* 7: 263.
3. André, P., C. Denis, C. Soulas, C. Bourbon-Caillet, J. Lopez, T. Arnoux, M. Blery, C. Bonnafous, L. Gauthier, A. Morel, B. Rossi, et al. 2018. Anti-NKG2A mAb is a checkpoint inhibitor that promotes anti-tumor immunity by unleashing both T and NK cells. *Cell* 175: 1731–1743.13.
4. van Montfoort, N., L. Borst, M. J. Korrer, M. Sluijter, K. A. Marijt, S. J. Santegoets, V. J. van Ham, I. Ehsan, P. Charoentong, P. Andre, et al. 2018. NKG2A blockade potentiates CD8 T cell immunity induced by cancer vaccines. *Cell* 175: 1744–1755.e15.
5. Imani, F., and M. J. Soloski. 1991. Heat shock proteins can regulate expression of the Tla region-encoded class Ib molecule Qa-1. *Proc. Natl. Acad. Sci. USA* 88: 10475–10479.
6. Ohtsuka, M., H. Inoko, J. K. Kulski, and S. Yoshimura. 2008. *Major histocompatibility complex* (*Mhc*) class Ib gene duplications, organization and expression patterns in mouse strain C57BL/6. *BMC Genomics* 9: 178.
7. DeCloux, A., A. S. Woods, R. J. Cotter, M. J. Soloski, and J. Forman. 1997. Dominance of a single peptide bound to the class I(B) molecule, Qa-1b. *J. Immunol.* 158: 2183–2191.
8. Bai, A., J. Broen, and J. Forman. 1998. The pathway for processing leader-derived peptides that regulate the maturation and expression of Qa-1b. *Immunity* 9: 413–421.
9. Oliveira, C. C., P. A. van Veelen, B. Querido, A. de Ru, M. Sluijter, S. Laban, J. W. Drijfhout, S. H. van der Burg, R. Offringa, and T. van Hall. 2010. The nonpolymorphic MHC Qa-1b mediates CD8$^+$ T cell surveillance of antigen-processing defects. [Published erratum appears in 2010 *J. Exp. Med.* 207: 671.] *J. Exp. Med.* 207: 207–221.
10. Kambayashi, T., J. R. Kraft-Leavy, J. G. Dauner, B. A. Sullivan, O. Laur, and P. E. Jensen. 2004. The nonclassical MHC class I molecule Qa-1 forms unstable peptide complexes. *J. Immunol.* 172: 1661–1669.
11. Zeng, L., L. C. Sullivan, J. P. Vivian, N. G. Walpole, C. M. Harpur, J. Rossjohn, C. S. Clements, and A. G. Brooks. 2012. A structural basis for antigen presentation by the MHC class Ib molecule, Qa-1b. *J. Immunol.* 188: 302–310.
12. Salcedo, M., P. Bousso, H. G. Ljunggren, P. Kourilsky, and J. P. Abastado. 1998. The Qa-1b molecule binds to a large subpopulation of murine NK cells. *Eur. J. Immunol.* 28: 4356–4361.

13. Houchins, J. P., L. L. Lanier, E. C. Niemi, J. H. Phillips, and J. C. Ryan. 1997. Natural killer cell cytolytic activity is inhibited by NKG2-A and activated by NKG2-C. *J. Immunol.* 158: 3603–3609.
14. Le Dréan, E., F. Vély, L. Olcese, A. Cambiaggi, S. Guia, G. Krystal, N. Gervois, A. Moretta, F. Jotereau, and E. Vivier. 1998. Inhibition of antigen-induced T cell response and antibody-induced NK cell cytotoxicity by NKG2A: association of NKG2A with SHP-1 and SHP-2 protein-tyrosine phosphatases. *Eur. J. Immunol.* 28: 264–276.
15. Carretero, M., G. Palmieri, M. Llano, V. Tullio, A. Santoni, D. E. Geraghty, and M. López-Botet. 1998. Specific engagement of the CD94/NKG2-A killer inhibitory receptor by the HLA-E class Ib molecule induces SHP-1 phosphatase recruitment to tyrosine-phosphorylated NKG2-A: evidence for receptor function in heterologous transfectants. *Eur. J. Immunol.* 28: 1280–1291.
16. Chen, Y., Z. Xin, L. Huang, L. Zhao, S. Wang, J. Cheng, P. Wu, and Y. Chai. 2020. $CD8^+$ T cells form the predominant subset of $NKG2A^+$ cells in human lung cancer. *Front. Immunol.* 10: 3002.
17. Abd Hamid, M., R. Z. Wang, X. Yao, P. Fan, X. Li, X. M. Chang, Y. Feng, S. Jones, D. Maldonado-Perez, C. Waugh, et al. 2019. Enriched HLA-E and CD94/NKG2A interaction limits antitumor $CD8^+$ tumor-infiltrating T lymphocyte responses. *Cancer Immunol. Res.* 7: 1293–1306.
18. Sivakumar, P. V., A. Gunturi, M. Salcedo, J. D. Schatzle, W. C. Lai, Z. Kurepa, L. Pitcher, M. S. Seaman, F. A. Lemonnier, M. Bennett, et al. 1999. Cutting edge: expression of functional CD94/NKG2A inhibitory receptors on fetal $NK1.1^+Ly\text{-}49^-$ cells: a possible mechanism of tolerance during NK cell development. *J. Immunol.* 162: 6976–6980.
19. Toyama-Sorimachi, N., Y. Taguchi, H. Yagita, F. Kitamura, A. Kawasaki, S. Koyasu, and H. Karasuyama. 2001. Mouse CD94 participates in Qa-1-mediated self recognition by NK cells and delivers inhibitory signals independent of Ly-49. *J. Immunol.* 166: 3771–3779.
20. Persson, C. M., E. Assarsson, G. Vahlne, P. Brodin, and B. J. Chambers. 2008. Critical role of Qa1b in the protection of mature dendritic cells from NK cell-mediated killing. *Scand. J. Immunol.* 67: 30–36.
21. Colmenero, P., A. L. Zhang, T. Qian, L. Lu, H. Cantor, K. Söderström, and E. G. Engleman. 2007. Qa-1^b-dependent modulation of dendritic cell and NK cell cross-talk in vivo. *J. Immunol.* 179: 4608–4615.
22. Lu, L., K. Ikizawa, D. Hu, M. B. Werneck, K. W. Wucherpfennig, and H. Cantor. 2007. Regulation of activated $CD4^+$ T cells by NK cells via the Qa-1-NKG2A inhibitory pathway. *Immunity* 26: 593–604.
23. Seaman, M. S., B. Pérarnau, K. F. Lindahl, F. A. Lemonnier, and J. Forman. 1999. Response to *Listeria monocytogenes* in mice lacking MHC class Ia molecules. *J. Immunol.* 162: 5429–5436.
24. Lo, W. F., H. Ong, E. S. Metcalf, and M. J. Soloski. 1999. T cell responses to Gram-negative intracellular bacterial pathogens: a role for $CD8^+$ T cells in immunity to *Salmonella* infection and the involvement of MHC class Ib molecules. *J. Immunol.* 162: 5398–5406.
25. Weidanz, J. A., O. Hawkins, B. Verma, and W. H. Hildebrand. 2011. TCR-like biomolecules target peptide/MHC class I complexes on the surface of infected and cancerous cells. *Int. Rev. Immunol.* 30: 328–340.
26. Dahan, R., and Y. Reiter. 2012. T-cell-receptor-like antibodies—generation, function and applications. *Expert Rev. Mol. Med.* 14: e6.
27. Chang, A. Y., R. S. Gejman, E. J. Brea, C. Y. Oh, M. D. Mathias, D. Pankov, E. Casey, T. Dao, and D. A. Scheinberg. 2016. Opportunities and challenges for TCR mimic antibodies in cancer therapy. *Expert Opin. Biol. Ther.* 16: 979–987.
28. Pardon, E., T. Laeremans, S. Triest, S. G. Rasmussen, A. Wohlkönig, A. Ruf, S. Muyldermans, W. G. Hol, B. K. Kobilka, and J. Steyaert. 2014. A general protocol for the generation of Nanobodies for structural biology. *Nat. Protoc.* 9: 674–693.
29. Van Deventer, J. A., and K. D. Wittrup. 2014. Yeast surface display for antibody isolation: library construction, library screening, and affinity maturation. *Methods Mol. Biol.* 1131: 151–181.
30. Doorduijn, E. M., M. Sluijter, B. J. Querido, U. J. E. Seidel, C. C. Oliveira, S. H. van der Burg, and T. van Hall. 2018. T cells engaging the conserved MHC class Ib molecule Qa-1^b with TAP-independent peptides are semi-invariant lymphocytes. *Front. Immunol.* 9: 60.
31. Cotterill, L. A., H. J. Stauss, M. M. Millrain, D. J. Pappin, D. Rahman, B. Canas, P. Chandler, A. Stackpoole, E. Simpson, P. J. Robinson, and P. J. Dyson. 1997. Qa-1 interaction and T cell recognition of the Qa-1 determinant modifier peptide. *Eur. J. Immunol.* 27: 2123–2132.
32. Kurepa, Z., and J. Forman. 1997. Peptide binding to the class Ib molecule, Qa-1b. *J. Immunol.* 158: 3244–3251.
33. Kraft, J. R., R. E. Vance, J. Pohl, A. M. Martin, D. H. Raulet, and P. E. Jensen. 2000. Analysis of Qa-1^b peptide binding specificity and the capacity of CD94/NKG2A to discriminate between Qa-1-peptide complexes. *J. Exp. Med.* 192: 613–624.
34. Neethling, F. A., V. Ramakrishna, T. Keler, R. Buchli, T. Woodburn, and J. A. Weidanz. 2008. Assessing vaccine potency using TCRmimic antibodies. *Vaccine* 26: 3092–3102.
35. Kaabinejadian, S., C. P. McMurtrey, S. Kim, R. Jain, W. Bardet, F. B. Schafer, J. L. Davenport, A. D. Martin, M. S. Diamond, J. A. Weidanz, et al. 2016. Immunodominant West Nile virus T cell epitopes are fewer in number and fashionably late. *J. Immunol.* 196: 4263–4273.
36. Patterson, A. M., S. Kaabinejadian, C. P. McMurtrey, W. Bardet, K. W. Jackson, R. E. Zuna, S. Husain, G. P. Adams, G. MacDonald, R. L. Dillon, et al. 2016. Human leukocyte antigen-presented macrophage migration inhibitory factor is a surface biomarker and potential therapeutic target for ovarian cancer. *Mol. Cancer Ther.* 15: 313–322.
37. Weidanz, J. A., T. Nguyen, T. Woodburn, F. A. Neethling, M. Chiriva-Internati, W. H. Hildebrand, and J. Lustgarten. 2006. Levels of specific peptide-HLA class I complex predicts tumor cell susceptibility to CTL killing. *J. Immunol.* 177: 5088–5097.
38. Zehn, D., C. J. Cohen, Y. Reiter, and P. Walden. 2004. Extended presentation of specific MHC-peptide complexes by mature dendritic cells compared to other types of antigen-presenting cells. *Eur. J. Immunol.* 34: 1551–1560.
39. Weidanz, J. A., P. Piazza, H. Hickman-Miller, D. Woodburn, T. Nguyen, A. Wahl, F. Neethling, M. Chiriva-Internati, C. R. Rinaldo, and W. H. Hildebrand. 2007. Development and implementation of a direct detection, quantitation and validation system for class I MHC self-peptide epitopes. *J. Immunol. Methods* 318: 47–58.
40. Dass, S. A., M. N. Norazmi, A. A. Dominguez, M. E. S. G. S. Miguel, and G. J. Tye. 2018. Generation of a T cell receptor (TCR)-like single domain antibody (sDAb) against a *Mycobacterium tuberculosis* (Mtb) heat shock protein (HSP) 16kDa antigen presented by human leukocyte antigen (HLA)-A*02. *Mol. Immunol.* 101: 189–196.
41. Zhang, G., R. Liu, X. Zhu, L. Wang, J. Ma, H. Han, X. Wang, G. Zhang, W. He, W. Wang, et al. 2013. Retargeting NK-92 for anti-melanoma activity by a TCR-like single-domain antibody. *Immunol. Cell Biol.* 91: 615–624.
42. Holland, C. J., R. M. Crean, J. M. Pentier, B. de Wet, A. Lloyd, V. Srikannathasan, N. Lissin, K. A. Lloyd, T. H. Blicher, P. J. Conroy, et al. 2020. Specificity of bispecific T cell receptors and antibodies targeting peptide-HLA. *J. Clin. Invest.* 130: 2673–2688.
43. Muyldermans, S. 2013. Nanobodies: natural single-domain antibodies. *Annu. Rev. Biochem.* 82: 775–797.
44. Aldrich, C. J., A. DeCloux, A. S. Woods, R. J. Cotter, M. J. Soloski, and J. Forman. 1994. Identification of a Tap-dependent leader peptide recognized by alloreactive T cells specific for a class Ib antigen. *Cell* 79: 649–658.
45. Chun, T., C. J. Aldrich, M. E. Baldeón, L. V. Kawczynski, M. J. Soloski, and H. R. Gaskins. 1998. Constitutive and regulated expression of the class IB molecule Qa-1 in pancreatic beta cells. *Immunology* 94: 64–71.
46. Xu, H. C., J. Huang, A. A. Pandyra, E. Lang, Y. Zhuang, C. Thöns, J. Timm, D. Häussinger, M. Colonna, H. Cantor, et al. 2017. Lymphocytes negatively regulate NK cell activity via Qa-1b following viral infection. *Cell Rep.* 21: 2528–2540.
47. Ferez, M., C. J. Knudson, A. Lev, E. B. Wong, P. Alves-Peixoto, L. Tang, C. Stotesbury, and L. J. Sigal. 2021. Viral infection modulates Qa-1b in infected and bystander cells to properly direct NK cell killing. *J. Exp. Med.* 218: e20201782 .
48. Zhou, J., M. Matsuoka, H. Cantor, R. Homer, and R. I. Enelow. 2008. Cutting edge: engagement of NKG2A on $CD8^+$ effector T cells limits immunopathology in influenza pneumonia. *J. Immunol.* 180: 25–29.
49. Vance, R. E., J. R. Kraft, J. D. Altman, P. E. Jensen, and D. H. Raulet. 1998. Mouse CD94/NKG2A is a natural killer cell receptor for the nonclassical major histocompatibility complex (MHC) class I molecule Qa-1^b. *J. Exp. Med.* 188: 1841–1848.
50. Vance, R. E., A. M. Jamieson, and D. H. Raulet. 1999. Recognition of the class Ib molecule Qa-1^b by putative activating receptors CD94/NKG2C and CD94/NKG2E on mouse natural killer cells. *J. Exp. Med.* 190: 1801–1812.